SUPPLEMENTAL DATA

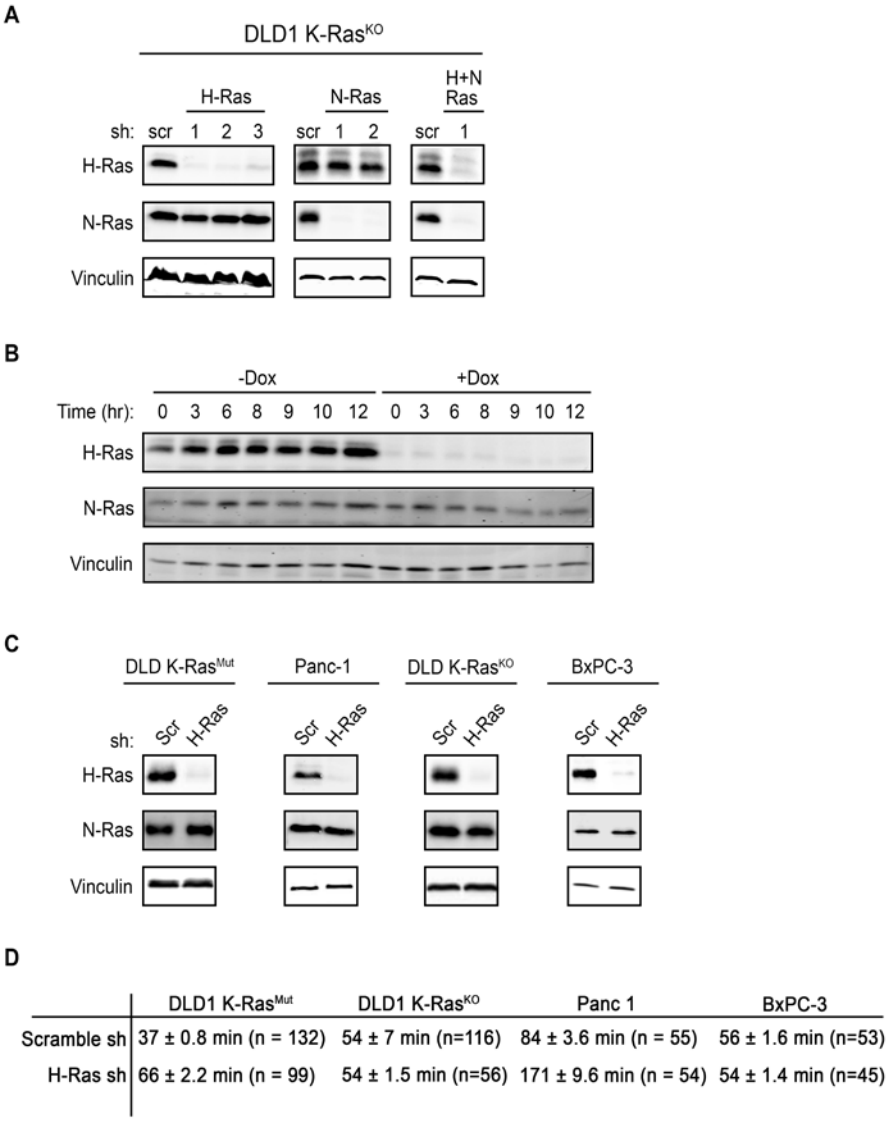

	DLD1 K-Ras^{Mut}	DLD1 K-Ras^{KO}	Panc 1	BxPC-3
Scramble sh	37 ± 0.8 min (n = 132)	54 ± 7 min (n=116)	84 ± 3.6 min (n = 55)	56 ± 1.6 min (n=53)
H-Ras sh	66 ± 2.2 min (n = 99)	54 ± 1.5 min (n=56)	171 ± 9.6 min (n = 54)	54 ± 1.4 min (n=45)

Figure S1 related to Figure 1. Targeted knockdown of WT-H-Ras, WT-N-Ras, or WT-H-Ras and WT-N-Ras combined. (A) Knockdown of WT-H-Ras, WT-N-Ras, or WT-H-Ras and WT-N-Ras combined in DLD1 K-Ras^{KO} cancer cells corresponding to Figure 1D.

(B) Knockdown of WT-H-Ras in DLD1 K-Ras^{Mut} cancer cells released from a double thymidine block corresponding to Figure 1E-G.

(C) Knockdown of WT-H-Ras in DLD1 K-Ras^{Mut}, Panc-1, DLD1 K-Ras^{KO}, and BxPC-3 cancer cells corresponding to Figure 1H.

(D) Quantification of the duration of mitosis in DLD1 K-Ras^{Mut}, Panc-1, DLD1 K-Ras^{KO}, and BxPC-3 cells as shown in Figure 1H.

Movie S1 related to Figure 1. Mitotic progression in Panc-1 cells. Panc-1 cells induced to express a scramble shRNA were monitored every 7 min for a period of 16 hr. Time is shown in hr : min. Mitosis was tracked from prophase, just before nuclear envelope breakdown (NEB), until cytokinesis and partitioning of the cytoplasm.

Movie S2 related to Figure 1. K-Ras mutant cancer cells require WT-H-Ras for the timely progression through mitosis. Panc-1 cells induced to express a WT-H-Ras shRNA were monitored as in Supplementary Movie 1. Most WT-H-Ras ablated cells were delayed in prometaphase/metaphase, and took on average 2-3 times longer to progress to anaphase. A similar delay was also observed in anaphase/cytokinesis completion. This delay, together with the chromatin aberrations observed, similar to those shown for DLD1-K-Ras^{Mut} cells in Figure 1G, suggest a failure to satisfy the spindle assembly checkpoint (SAC)

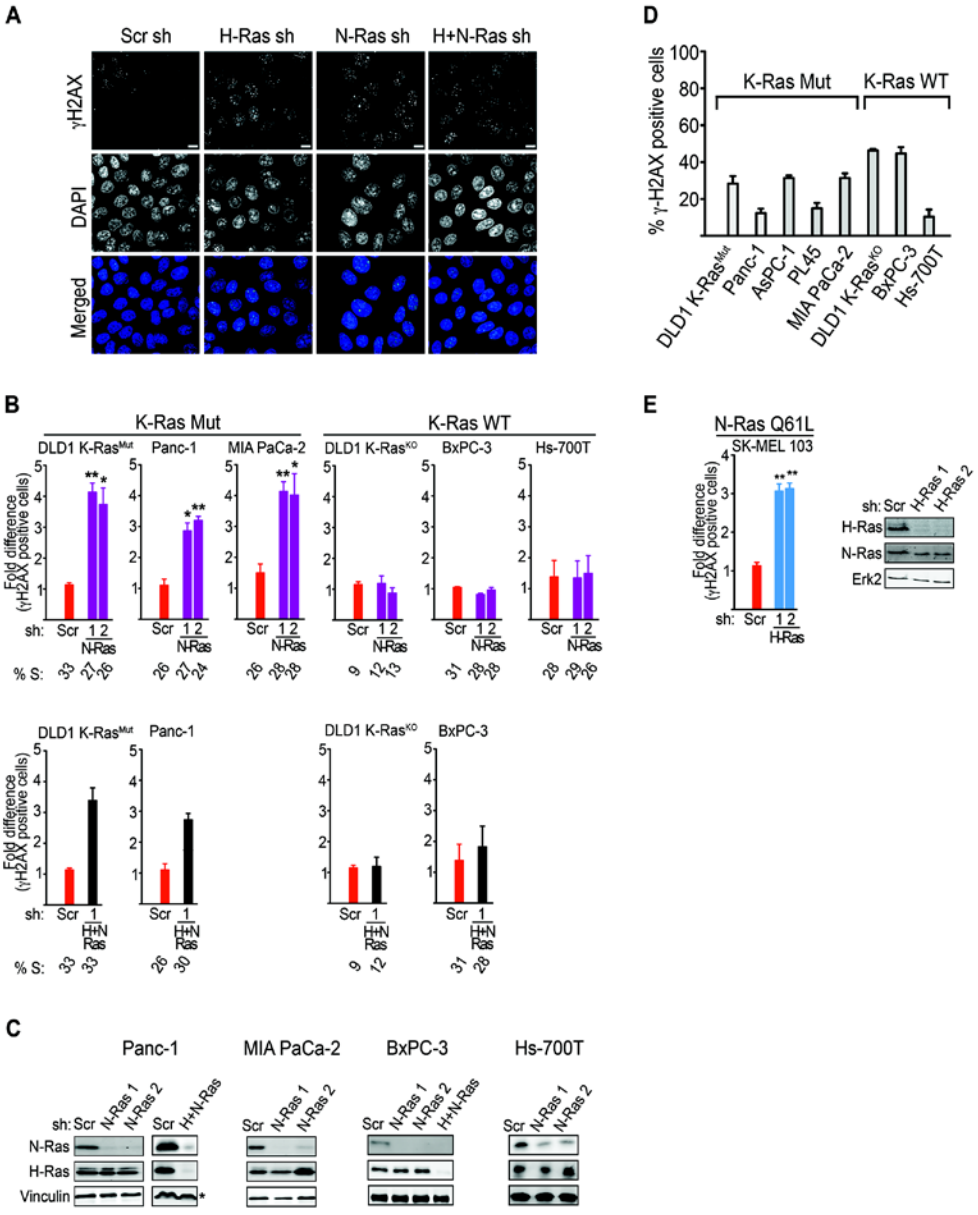

Figure S2 related to Figure 2. Knockdown of WT-H-Ras, WT-N-Ras, or both WT-H-Ras and WT-N-Ras, enhance DNA damage specifically in K-Ras mutant cancer cells.

(A) Representative images showing enhancement of γH2AX positive cells in WT-H-Ras, WT-N-Ras, or both WT-H-Ras and WT-N-Ras-suppressed DLD1 K-Ras^{Mut} cells. Cells were co-stained for γH2AX (green) and DAPI (blue). Scale bars, 5 μm.

(B) Quantification of γH2AX positive cells (foci >10 per cell) in K-Ras Mut and K-Ras WT cancer cells depleted of WT-N-Ras alone or combined with WT-H-Ras. S-phase percentages as determined by flow cytometry analysis of the percentage of BrdU-incorporating cells are indicated below the bar graphs.

(C) Knockdown of WT-N-Ras or H- and N-Ras combined in Panc-1, MIA PaCa-2, BxPC-3, and Hs-700T cells. See Figure 1A and Figure S1A for DLD1 K-Ras^{Mut} and DLD1 K-Ras^{KO}. Immunoblots for N-Ras, H-Ras, and vinculin as loading control are shown; * denotes tubulin as loading control.

(D) Percentage of γH2AX positive cells in cancer cell lines utilized in this study. The indicated cell lines were fixed, stained for γH2AX and DAPI, and the percentage of γH2AX positive cells (>10 foci per cell) was determined. Data are representative of 3 independent experiments.

(E) Quantification of γH2AX positive cells in N-Ras mutant cancer cells (SK-MEL 103) upon WT-H-Ras knockdown. Immunoblots for N-Ras, H-Ras, and Erk2 as loading control are shown. (B and E) Error bars, mean ± SEM, n=3 with at least 500 cells scored per experiment. Data are presented relative to the values obtained for scramble shRNA cells in each cell line, respectively. *$p<0.05$, **$p<0.005$.

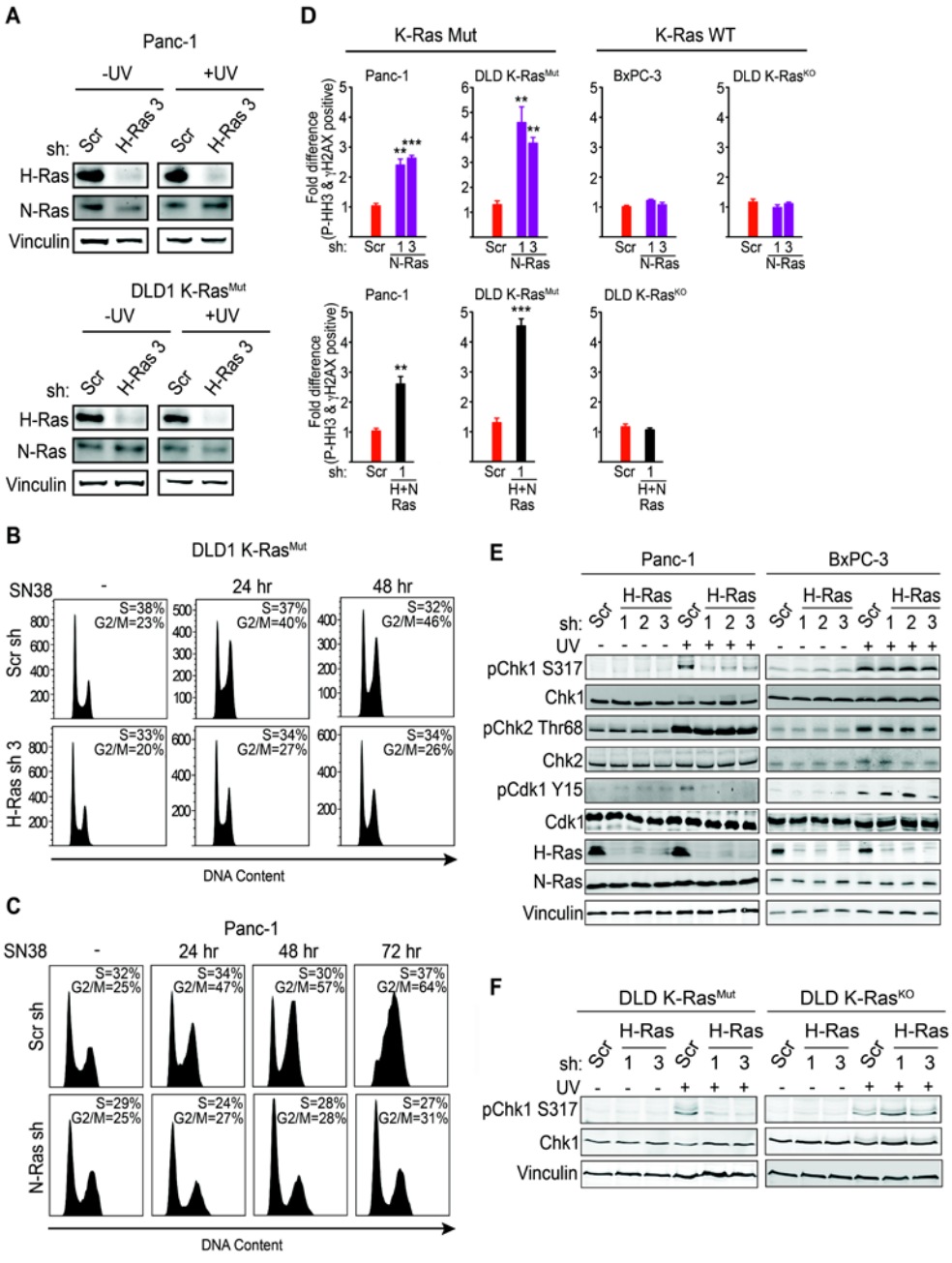
A
Panc-1
-UV
+UV
sh: Scr H-Ras 3 Scr H-Ras 3
H-Ras
N-Ras
Vinculin
DLD1 K-Ras^Mut
-UV
+UV
sh: Scr H-Ras 3 Scr H-Ras 3
H-Ras
N-Ras
Vinculin
D
K-Ras Mut
K-Ras WT
Panc-1
DLD K-Ras^Mut
BxPC-3
DLD K-Ras^KO
Fold difference (P-HH3 & γH2AX positive)
sh: Scr 1 3
N-Ras
Panc-1
DLD K-Ras^Mut
DLD K-Ras^KO
Fold difference (P-HH3 & γH2AX positive)
sh: Scr 1
H+N Ras
B
DLD1 K-Ras^Mut
SN38 - 24 hr 48 hr
Scr sh
H-Ras sh 3
S=38% G2/M=23%
S=37% G2/M=40%
S=32% G2/M=46%
S=33% G2/M=20%
S=34% G2/M=27%
S=34% G2/M=26%
DNA Content
C
Panc-1
SN38 - 24 hr 48 hr 72 hr
Scr sh
N-Ras sh
S=32% G2/M=25%
S=34% G2/M=47%
S=30% G2/M=57%
S=37% G2/M=64%
S=29% G2/M=25%
S=24% G2/M=27%
S=28% G2/M=28%
S=27% G2/M=31%
DNA Content
E
Panc-1
BxPC-3
H-Ras
sh: Scr 1 2 3 Scr 1 2 3
UV
pChk1 S317
Chk1
pChk2 Thr68
Chk2
pCdk1 Y15
Cdk1
H-Ras
N-Ras
Vinculin
F
DLD K-Ras^Mut
DLD K-Ras^KO
H-Ras
sh: Scr 1 3 Scr 1 3
UV
pChk1 S317
Chk1
Vinculin

Figure S3 related to Figure 3. WT-H-Ras and/or WT-N-Ras knockdown abrogates the G2 DNA damage checkpoint selectively in K-Ras mutant cancer cell lines.

(A) Knockdown of WT-H-Ras in Panc-1 and DLD1 K-Ras^{Mut} cells after mock and UV-C irradiation (25 J/m^2 UV, 2 hr) corresponding to Figure 3A, B.

(B-C) FACS histograms showing that in response to treatment with SN38 (2 nM), DLD1 K-Ras^{Mut} cells depleted of WT-H-Ras (B) and Panc-1 cells depleted of WT-N-Ras (C) fail to establish a checkpoint response. The S and G2/M fractions are indicated. Data are representative of 3 independent experiments. Note that the data shown in C is the same experiment as in Figure 3C, therefore the same control appears in both figures.

(D) Knockdown of WT-N-Ras, or WT-H-Ras and WT-N-Ras combined, allows mitotic entry with DNA damage specifically in K-Ras mutant cancer cells. The indicated cell lines were treated with UV-C, placed in nocodazole containing media for 4 hr to trap mitotic cells, and co-stained for P-HH3 and γH2AX. Quantifications of the fraction of mitotic cells (P-HH3) that are positive for γH2AX foci (>10 per cell) are shown. Data are presented as relative to the values obtained for scramble shRNA cells. Error bars, mean ± SEM, n=3 with at least 50 mitotic cells analyzed per experiment, **p<0.005, ***p<0.0005.

(E-F) Knockdown of WT-H-Ras impairs Chk1 activation in response to UV-C treatment in K-Ras Mut (Panc-1 and DLD1 K-Ras^{Mut}) but not in K-Ras WT (BxPC-3 and DLD1 K-Ras^{KO}) cells. Representative immunoblots (n=3) following mock ($^-$) or UV-C irradiation ($^+$) (25 J/m2, 2 hr) are shown.

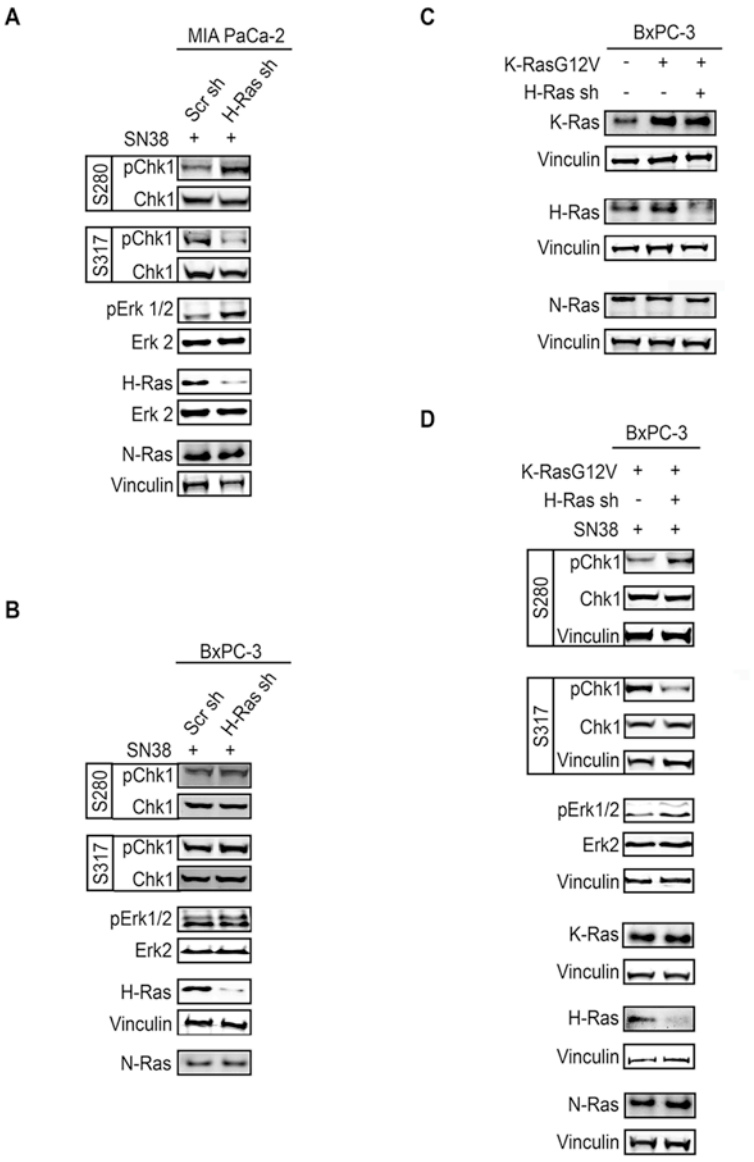

Figure S4 related to Figure 4. WT-H-Ras knockdown inhibits Chk1 activation in K-Ras mutant cells.

(A) WT-H-Ras knockdown impairs Chk1 activation in MIA PaCa-2 cells treated with SN38.

(B) WT-H-Ras knockdown has no effect on Chk1 activation in BxPC-3 cells treated with SN38**.**

(C) BxPC-3 cells engineered to inducibly express K-RasG12V alone or K-RasG12V and H-Ras sh were subjected to doxycycline for 96 hr, lysed and immunoblotted for K-Ras, H-Ras, N-Ras and the respective vinculin loading controls.

(D) BxPC-3 cells engineered to inducibly express K-RasG12V alone or K-RasG12V and H-Ras sh were subjected to doxycycline as indicated in B and treated with SN38 (8 nM) for 2 hr. Representative immunoblots show the levels of pChk1 Ser 280, pChk1 Ser 317, and the respective total Chk1; pErk1/2, total Erk2; K-Ras, H-Ras, N-Ras. Vinculin is shown as a loading control.

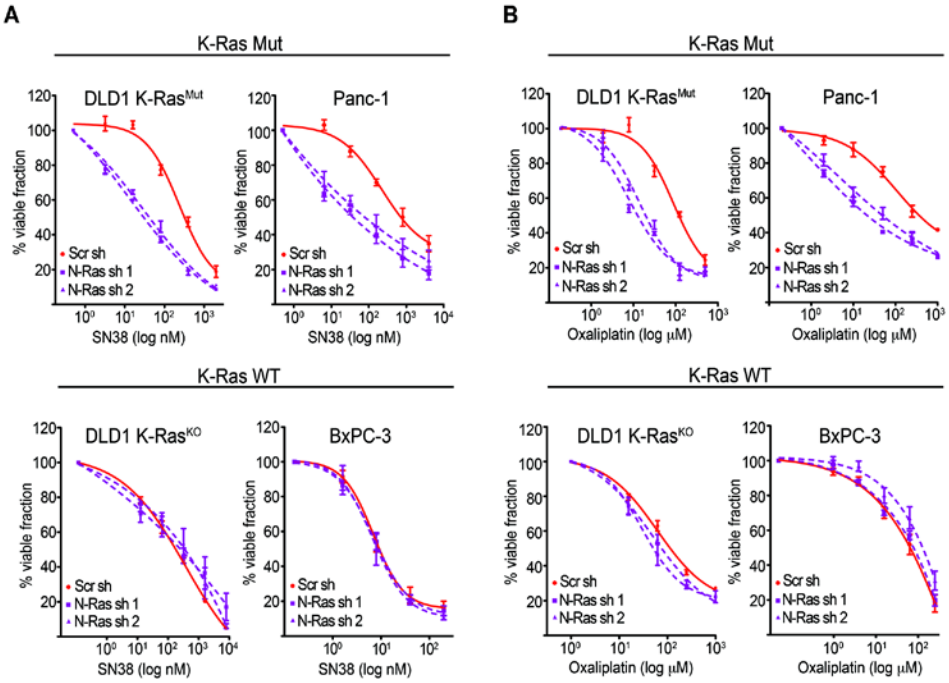

C

SN38 LogEC50 (nM)	Scramble sh	H-Ras sh 1	H-Ras sh 3	N-Ras sh 1	N-Ras sh 2
DLD1 K-Ras^{Mut}	2.4 -/+ 0.1	0.3 -/+ 0.2	0.8 -/+ 0.4	1.1 -/+ 0.1	1.2 -/+ 0.2
Panc-1	2.4 -/+ 0.2	0.8 -/+ 0.3	0.7 -/+ 0.6	0.9 -/+ 0.5	0.6 -/+ 0.5
DLD1 K-Ras^{KO}	2.6 -/+ 0.2	2.5 -/+ 0.1	2.6 -/+ 0.2	2.6 -/+ 0.9	2.4 -/+ 0.2
BxPC-3	0.9 -/+ 0.1	1.2 -/+ 0.1	1.1 -/+ 0.1	0.9 -/+ 0.1	0.8 -/+ 0.1

Oxaliplatin LogEC50 (μM)	Scramble sh	H-Ras sh 1	H-Ras sh 3	N-Ras sh 1	N-Ras sh 2
DLD1 K-Ras^{Mut}	2.0 -/+ 0.1	0.9 -/+ 0.1	0.9 -/+ 0.1	0.9 -/+ 0.1	1.2 -/+ 0.1
Panc-1	2.0 -/+ 0.1	0.6 -/+ 0.2	0.7 -/+ 0.4	0.4 -/+ 0.3	0.7 -/+ 0.6
DLD1 K-Ras^{KO}	1.8 -/+ 0.1	1.9 -/+ 0.1	2.0 -/+ 0.5	1.7 -/+ 0.1	1.8 -/+ 0.1
BxPC-3	2.8 -/+ 0.7	2.9 -/+ 1.1	2.7 -/+ 1.6	2.9 -/+ 0.8	3.2 -/+ 1.1

Figure S5 related to Figure 5. Sensitization of K-Ras mutant cancer cells depleted of WT-N-Ras to DNA damage inducing chemotherapeutic agents. (A-B) MTT cell viability assays of K-Ras Mut cancer cells (DLD1 K-Ras^{Mut} and Panc-1) and K-Ras WT cancer cells (DLD1 K-Ras^{KO} and BxPC-3) induced to

express scramble or WT-N-Ras shRNAs, and following a 72 hr treatment with SN38 (A) or oxaliplatin (B). Viable fraction is expressed as a percentage mean ± SEM of the viability values obtained for the respective untreated conditions (Scr sh, N-Ras sh 1, and N-Ras sh 2) from at least 3 independent experiments. $p<0.005$ comparing N-Ras sh 1 or N-Ras sh 2 plus SN-38 or oxaliplatin with Scr sh plus SN-38 or oxaliplatin, respectively.

(C) SN38 and Oxaliplatin EC50 values for K-Ras Mut and K-Ras WT cancer cells depleted of WT-H-Ras or WT-N-Ras.

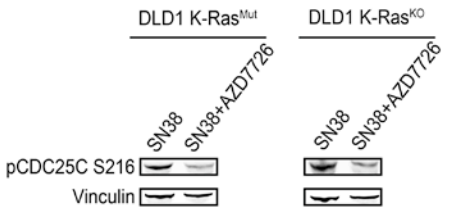

Figure S6 related to Figure 6. Inhibition of Chk1/Chk2 activity by AZD7762 treatment. DLD1 K-Ras^{Mut} and DLD1 K-Ras^{KO} cell lines were treated with SN38 and with and without AZD7762 (80 nM). Following 5 hr of simultaneous treatment, cells were harvested and whole cell lysates were analyzed for the activation status of the Chk1/Chk2 substrate CDC25C by immunoblotting with a pCDC25C S216 antibody.

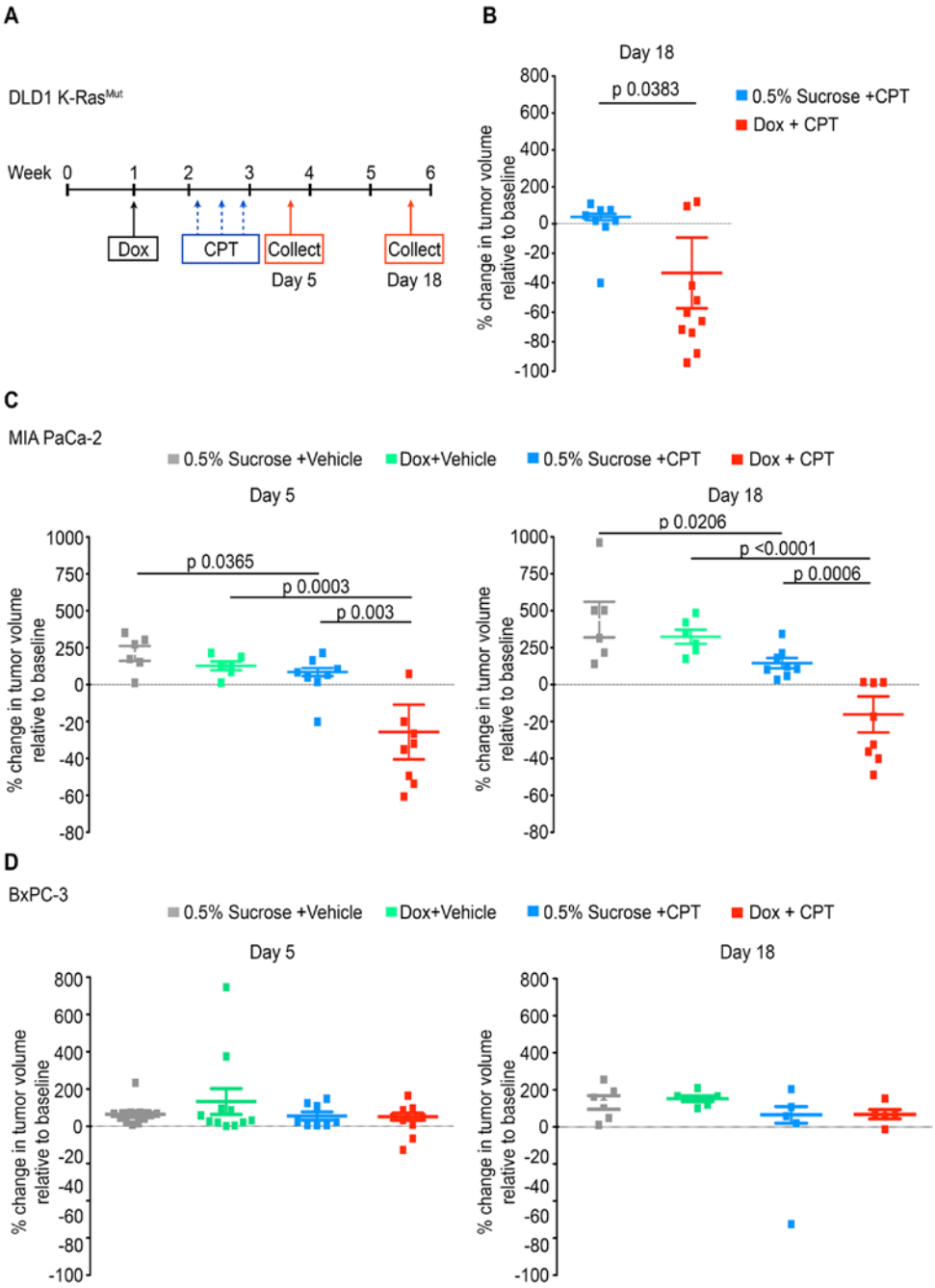

Figure S7 related to Figure 7. Combination of WT-H-Ras knockdown and irinotecan treatment leads to K-Ras mutant tumor regression.

(A-B) Schematic of treatment module for DLD1 K-Ras^{Mut} tumors (A) and scatter plot (B) showing percentage change in the volume of subcutaneous DLD1 K-Ras^{Mut} tumors in nude mice eighteen days after the last dose of irinotecan (CPT) administration.

(C-D) Percentage change in the volume of subcutaneous MIA PaCa-2 (K-Ras Mut) (C) and BxPC-3 (K-Ras WT) (D) tumors following irinotecan (CPT) administration.

All experiments: error bars, mean ± SEM.

SUPPLEMENTAL EXPERIMENTAL PROCEDURES

Plasmids and general reagents

The antibodies used for immunofluorescence, immunohistochemistry, and immunoblot analyses were from the following sources: anti-H-Ras (C-20), anti-N-Ras (F155), anti-K-Ras (F234), and anti-Chk1 were from Santa Cruz; anti-phospho-histone H2AX (γH2AX) and anti phospho-histone H3 (Ser 10) were from Millipore; anti-tubulin was from Sigma; anti-phospho-Chk1 (S317) was from Abcam; anti-ERK2, anti-phospho-Erk1/2 (Thr202/Tyr204), anti-Akt, anti-phospho-Akt (Ser473), anti-phospho cdc2 (Tyr 15), anti-Chk2, anti-phospho-Chk1 (S347), anti-phospho-Chk2 (Thr68), anti cdc2 were purchased from Cell Signaling. The DNA content dye for FACS analysis TO-PRO 3 was from Invitrogen. BrdU and anti-BrdU were from BD Transduction Labs. AZD7762 was from Selleck Chemicals. pLenti was from Addgene. The indicated shRNA sequences were cloned into the pTRIPZ lentiviral doxycycline inducible shRNA mir vector according to the manufacturer's protocol (Open Biosystems):

H-Ras 1 sh, 5'-GGCAAGAGTGCGCTGACCATC-3',

H-Ras 2 sh, 5'-CAGTACAGGGAGCAGATCAAA-3'

H-Ras 3 sh, 5'-CGGAAGCAGGTGGTCATTGAT-3'

N-Ras 1 sh, 5'-GGAGCAGATTAAGCGAGTAAA-3'

N-Ras 2 sh, 5'-AGAAATACGCCAGTACCGAAT-3'

Scramble sh, 5'-GGAAGTGCAATTATTCTATTA-3'

Cell growth assays

For growth assays, cells were treated with doxycycline to induce expression of the indicated shRNAs for 48 hr, and then seeded at a density of 500 cells/well in 96-well plates and maintained in doxycycline. At the times indicated, cells were fixed with 3.7% formaldehyde and stained with 1 μM Syto60 dye for 30 min. Fluorescence was quantified using the Odyssey infrared system (LiCor). Day 0 indicates cell number 24 hr post plating.

Ras activity assay and immunoblotting

The levels of GTP-loaded (active) Ras were determined by the GST-Ras-RBD pulldown assay, as previously described (Jeng et al., 2012). The proteins were detected by immunoblotting with the indicated antibodies. The levels of GTP-loaded H-Ras, N-Ras, or K-Ras were determined using the Odyssey infrared system (Li-Cor).

Immunofluorescence, immunohistochemistry, and live cell imaging

For immunofluorescence staining cells were grown on glass coverslips, fixed with ice-cold methanol and stained with the indicated primary antibodies for 1 hr at room temperature. Secondary antibodies goat anti-rabbit Alexa-350 and rabbit anti-mouse Alexa-488 were purchased from Invitrogen. We acquired immunofluorescence images using and Axiovert 200M (Zeiss) microscope controlled by AxioVision v4.7 (Zeiss) software. For UV-C irradiation experiments cells were treated with UV-C (25 J/m2) and placed in nocodazole (100 ng/ml, Sigma) containing media for 4 hr before fixation to trap mitotic cells. Immunohistochemistry was performed in sections from formalin-fixed paraffin-

embedded tissues as previously described (Pylayeva-Gupta et al., 2012). Sections were stained either with H&E to assess pathological appearance, or with rabbit anti-cleaved caspase 3 to determine apoptosis, or rabbit phospho histone H3 (Ser 10) to score mitotic cells. At least 3 xenografts with at least three 20X fields were scored for each treatment. Live cell imaging was conducted using a Zeiss Axiovert 200M equipped with a controlled temperature and CO_2 chamber to maintain 37°C and 5% CO_2 during acquisition. Images were acquired at 5 min intervals for DLD1 and BxPC-3 cell lines and 7 min intervals for Panc-1 cells for 16-20 hr. Duration of mitosis was scored from prophase, just before nuclear envelope breakdown (NEB) until cytokinesis and partitioning of the cytoplasm. AxioVision v4.7 (Zeiss) software was used for image acquisition and AxioVision v4.7 and Image J were used for image stack analysis and montage composition.

SUPPLEMENTAL REFERENCES

Jeng, H. H., Taylor, L. J., and Bar-Sagi, D. (2012). Sos-mediated cross-activation of wild-type Ras by oncogenic Ras is essential for tumorigenesis. Nature communications *3*, 1168.

Pylayeva-Gupta, Y., Lee, K. E., Hajdu, C. H., Miller, G., and Bar-Sagi, D. (2012). Oncogenic Kras-induced GM-CSF production promotes the development of pancreatic neoplasia. Cancer cell *21*, 836-847.